

Analysis of ECG and PCG Time Delay around Auscultation Sites

Xinqi Bao¹^a, Yansha Deng¹^b, Nicholas Gall²^c and Ernest Nlandu Kamavuako¹^d

¹Department of Engineering, King's College London, London, U.K.

²Department of Cardiology, King's College Hospital, London, U.K.

Xinqi.bao@kcl.ac.uk, Yansha.deng@kcl.ac.uk, Nickgall@doctors.org.uk, Ernest.kamavuako@kcl.ac.uk

Keywords: Phonocardiogram (PCG), Electrocardiogram (ECG), Auscultation Site, Time Delay.

Abstract: Phonocardiogram (PCG) and Electrocardiogram (ECG) are the two important signals for cardiac preliminary diagnosis. Using ECG as a reference for segmenting the PCG signal is a simple but reliable technique for the devices with integration capability of PCG and ECG recording. The aim of this work is to analyse the time delay between ECG and PCG at each auscultation site. To do so, we performed the experiments on 12 healthy subjects, where the ECG and PCG signals were collected simultaneously at two sites at each time. Our results reveal that 1) the inter-distance of the electrodes for ECG does not affect the occurrence time of the R-peak. 2) The delay between R-peak and onset of first heart sound (S1) depends on the auscultation site e.g. S1 onset occurs before the R-peak at auscultation site M. This study suggests that small integrated ECG-PCG devices can be made by reducing the distance between the ECG electrodes. In the meantime, distinguishing the auscultation location is necessary for performing more precise PCG segmentation using ECG as reference.


1 INTRODUCTION


Heart sound auscultation and Electrocardiogram (ECG) are the two most common and effective ways in the primary diagnosis of heart diseases. Their signal waveforms, phonocardiogram (PCG) and ECG can reflect the mechanical and electrical activities of the heart, respectively. The PCG signal can reveal the physiological or pathological conditions of cardiac valves and chambers to diagnose the structural heart disease (SHD), such as prolapsed mitral valve, ventricular septal defect (VSD), tricuspid regurgitation, etc. The ECG can help to detect diseases associated with impulse conduction, such as arrhythmias, coronary heart disease, heart attacks, etc. (Auer et al., 2012).


The normal cardiac cycle relies on the cooperation of electrical activity and mechanical contraction of the atria and ventricles of the heart. The whole process is initially stimulated by the spontaneous action potential in the sinoatrial (SA) node (represented as P wave on ECG), then propagated to the atrioventricular (AV) node causing the atria contraction and the blood is pumped into ventricles and the ventric-


ular depolarization (represented as QRS complex on ECG) begins. Once the ventricular pressure becomes greater than the atrial pressure, the atrioventricular valves close (represented as S1 onset on PCG) and the ventricular depolarization is finished. The continuation of the electrical signal goes through the bundle of His to the Purkinje fibres causing the ventricle contraction and the blood is pumped out of the heart. After the blood pumping out, the ventricles are repolarized (represented as T wave on PCG) and relaxed. The closure of the semilunar valves cause the S2 on the PCG. Therefore, the PCG and ECG are closely related in the time domain (Wartak, 1972).

In order to fully utilise the diagnosis power of the PCG, it is of utmost importance to segment S1 from S2. All the proposed segmentation methods can be basically grouped into: 1) ECG reference based methods use the R-peak and T wave to determine the locations of the heart sounds. It highly requires the simultaneous recording of the ECG and PCG signals (Lehner and Rangayyan, 1987; El-Segaier et al., 2005), but robust in performance and computationally efficient; 2) Envelope-based methods are more commonly used techniques in non-ECG based segmentation. They use the signal energy to do morphological transformation (Liang et al., 1997; Wang et al., 2009; Kang et al., 2015), but their performance decrease in the presence of large environmental noise and murmurs; 3) Temporal-spectral parameters based

^a  <https://orcid.org/0000-0002-7117-1267>

^b  <https://orcid.org/0000-0003-1001-7036>

^c  <https://orcid.org/0000-0003-1289-1421>

^d  <https://orcid.org/0000-0001-6846-2090>

methods use the time-frequency domain characteristics of the heart sounds, murmurs, and noise to segment the heart sound (Iwata et al., 1980; Liang et al., 1998); 4) Wavelet based PCG segmentation methods are the evolution of temporal-spectral parameters based methods (Oskiper and Watrous, 2002; Ölmez and Dokur, 2003; Kumar et al., 2006; Zhong et al., 2011). They will decompose the signals to emphasize the heart sounds and suppress the effects of murmurs and noises. The major challenge of wavelet-based segmentation method is to select the appropriate filters, decomposition level and required sub-bands for heart sound and murmurs detection; 5) Hidden Markov models are also used for segmentation in recent years (Ricke et al., 2005; Lima and Cardoso, 2007; Schmidt et al., 2010), and they have outstanding performance in low signal-to-noise ratio. At present, there is no widely recognized the best PCG segmentation method, but with the presence of simultaneous ECG recording, ECG-based segmentation is more desirable for practical applications due to its robustness and simplicity.

In the previous ECG-base PCG segmentation studies, S1 onset is conventionally considered to occur after R peak (Shino et al., 1996; Syed et al., 2004; Ahlström, 2006; Andresen et al., 2006). Ahlstrom (2006) detailedly summarized the time property of heart sounds that S1 starts 10–50 ms after R peak and lasts for 100–160 ms; S2 starts 280–360 ms after R-peak in ECG and lasts for 80–140 ms. For the practical applications, the development of microprocessor in the last two decades has made it possible to make portable devices that can be of great value in primary care. Devices, such as the SensiumVitals® system, Zio patch monitor and CAM patch monitor appear which can collect the ECG using a lightweight patch on the chest region. This provides the possibility to integrate ECG and PCG together around the chest auscultation area, instead of measuring at different place of the body. Integrating PCG and ECG together for concurrent measurement will be of great help to increase the portability and reduce the size in designing the small and portable device or systems. Furthermore, combining ECG with PCG can provide more comprehensive heart diagnosis (Phanphaisarn et al., 2011; Homaeinezhad et al., 2012; Zarrabi et al., 2017). In such case, the need for sophisticated segmentation can be mitigated by using the ECG as reference signal and segmenting the PCG accordingly.

To the best of our knowledge, research on automatic analysis of PCG is mainly based on single channel signals and the time correlation described is not exhaustive on which lead of ECG and auscultation site were used. However, multiple channels

auscultation will provide more comprehensive information on the heart conditions. On this basis, there are studies on multi-site PCG recording to visualize the heart related acoustic sounds by cardiac acoustic mapping (Okada, 1982; Cozic et al., 1998; Bahadirlar and Gülçür, 2000; Nogata et al., 2012; Sapsanis et al., 2018). These studies not only provide a new way to analyse the heart sound, but also illustrate that the heart sound generation and propagation delay in the auscultation area. In addition, the ECG signals have morphological changes due to the electrode placement around the chest. According to Kania (2014), the QRS complex shifts due to the electrodes placement (Kania et al., 2014). Therefore, it is not known whether the correlation between ECG and PCG remains the same when multiple channel signals are collected from different auscultations sites. In the case of small-scale ECG-PCG device, the recordings of the ECG should occur around the auscultation site. It is therefore of utmost importance to revisit the time properties of ECG and PCG.

The primary aim of this study is to analyse the time delay between ECG and PCG at different auscultation sites (A, P, T, M). The secondary aim is to investigate the changes in the time occurrence of the R-peak in relation to the distance between the recording electrodes. All the findings will contribute to design small-scale ECG-PCG integrated device and provide more precise time property for ECG-based PCG segmentation.

2 METHODOLOGY

2.1 Experiment

2.1.1 Subjects

The experiments were conducted on 12 human subjects with no history of heart diseases (8 male/ 4 female, age range 21–28 years, mean 25.6 years). The procedures were approved by the King's College Research Ethics Committee (Approval No.: LRS-18/19-10673). Subjects gave written informed consent prior to the experimental procedures.

2.1.2 Data Collection

The proposed experiment requires the simultaneous acquisition of ECG and PCG signals at each auscultation site. A simple block diagram of this hardware system is shown in Figure 1. The recording uses the commercial acquisition system (iWorx, model RA

834) as recorder. ECG devices (iWire-BIO4) and digital stethoscopes (ThinkLab One) are connected with the recorder by iWire inputs and DIN8 inputs. The solid gel electrodes (Ambu 0215M) are used as ECG sensors. The sampling frequency was 20 kHz to allow fine resolution around the 0.05 ms. The filter for ECG was 0.05 – 40 Hz (Ricciardi et al., 2016), and PCGs were recorded with wideband mode (20 – 2000 Hz).

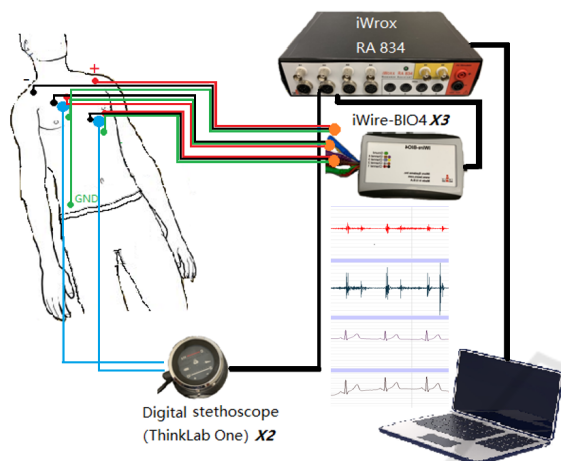


Figure 1: Block Diagram of the recording setup.

2.1.3 Experimental Procedures

Prior to commencing the experiments, we quantified the instrumentation delay. To achieve this, all three iWire devices were connected to the same electrodes in a limb lead configuration while both microphones were placed close to the auscultation site A. The sampling frequency was set to 100 KHz for this particular measurement. Instrumentation delay was very negligible about 10 microseconds.

The experiments are divided into two stages, and the subjects should keep supine. Stage I is to analyse whether the inter-electrode distance (IED) will affect the ECG delays. Three groups of disposable adhesive ECG sensors are placed at A site with 5 cm, 10 cm and 15 cm IED as shown in Figure 2 (a). The data is collected for 3 mins.

In Stage II, the effect of placement on ECG and PCG delays will be analysed. Three electrodes (red points) are positioned over the chest of a subject with standard Lead I as reference. The other two iWire devices will do the simultaneous recording with 10 cm IED at each auscultation site. Two ThinkLab stethoscopes are put at the centre of the electrodes (auscultation points). Each site is identified using the anatomical landmark and listening. The placement of sensors in Stage II can be seen in Figure 2 (b). Four groups of data are collected corresponding to each auscultation site with 3 mins duration.

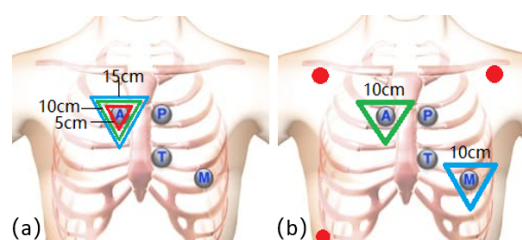


Figure 2: (a) Placement of electrodes for different inter-electrode distance (IED). (b) Placement of sensors for different auscultation locations.

2.2 Data Analysis

In this study, the delays were analysed using the temporal locations of the R-peaks, the Q points and the T wave ending points in ECG, and the S1, S2 starting points in PCG. The processing was conducted in the Matlab® R2018b environment.

2.2.1 Signal Filtering

The captured ECG and PCG signals were filtered first to remove the unwanted noise. For the ECG, a 3rd-order infinite impulse response (IIR) high-pass filter with 1 Hz is used to eliminate the baseline wander (Laguna et al., 1992). For the PCG, a 150 Hz low-pass IIR Chebyshev type I filter of order 3 is used to filter the lung sound. All filters were zero-phased.

2.2.2 Parameter Extraction

As mentioned in 2.2, the R-peaks, Q points and the T wave ending points are extracted from ECG signals, and S1, S2 starting points are extracted from PCG signals. Figure 3 shows the extraction results of the parameters.

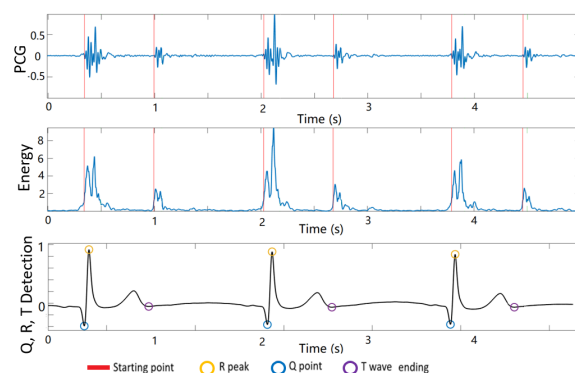


Figure 3: The S1, S2 starting points in PCG, and Q, R, T points in ECG extraction result.

To capture more accurate R-peak, the Pan-Tompkins algorithm (Pan and Tompkins, 1985) is

used. The ECG signal is derivative filtered and squared to enhance the dominant peaks (QRSs) and reduce the possibility of erroneously recognizing a T-wave as an R-peak. After the square, the R peaks of the ECG can be easily detected by setting an appropriate threshold. By using the intermediate coordinates between the R peaks, the ECG and corresponding PCG can be cut into one cardiac cycle. The data will be analyzed using 5 consecutive cycles. The Q points are detected by calculating the slope on the left side of R. When the slope (first derivative) is becoming greater than or equal to 0, the first lowest point is reached, which is the Q point. The detection of T wave ending point is based on the relationship between R peak and T wave, where T wave normally occurs 250 ms – 350 ms after R peak (O’Keefe Jr et al., 2010). Therefore, the peak point in this period is the T peak, and then we use the same method of Q detection to find T ending point by the first derivative.

For S1, S2 starting point detection, the short-term energy (STE) method (Malarvili et al., 2003) is used. Its equation is

$$E_n = \sum_{m=0}^{N-1} x_n^2(m), \quad (1)$$

where E_n is the short-term energy of the signal X_n at frame n , and N is the length of the frame. In our study, the frame length is 10 ms, and frame increase is 0.5 ms. There are two thresholds to determine whether the sound is a heart sound or noise: energy threshold and duration threshold. If the STE is larger than the lower energy threshold (10% of the maximum energy), it is regarded as the potential start point. When it becomes larger than the higher energy threshold (25% of the maximum energy) and its duration is longer than the threshold, this sound will be regarded as heart sound.

After the parameter extraction, the captured data are shown in Table 1. It worth mentioning that during the parameter extraction, manual check is also used to reduce the error and enhance its accuracy.

2.2.3 ECG Delay Estimation Method

In this study, the Cross-correlation (CC) method is used for ECG delay estimation. CC is a function to measure the similarity of two signals by calculating the sliding inner-product, which is given as:

$$(s_1 * s_2)[\tau] \triangleq \sum_{m=-\infty}^{\infty} \overline{s_1[m]} s_2[t + \tau], \quad (2)$$

where s_1 and s_2 are the two signals to be compared, $\overline{s_1[m]}$ is the complex conjugate of $s_1[m]$, and τ is the displacement for inner-product. When $(s_1 * s_2)$ is the

Table 1: Extracted data from ECG and PCG. The subscripts (Ref, A, P, T, M) mean the data is collected by the placement of the electrodes in standard Lead I or around auscultation sites.

ECG	R peak	Q point
ECG _{ref}	R _{ref}	Q _{ref}
ECG _A	R _A	Q _A
ECG _P	R _P	Q _P
ECG _T	R _T	Q _T
ECG _M	R _M	Q _M
T ending point	S1 starting point	S2 starting point
T _{ref}	–	–
T _A	S1 _A	S2 _A
T _P	S1 _P	S2 _P
T _T	S1 _T	S2 _T
T _M	S1 _M	S2 _M

largest, it means the similarity is the greatest. For the ECG signals, they are regular and periodic, so the displacement to get the maximum CC is equivalent to the delay between the two signals. Using this relation, the time delay between the two ECG signals can be determined by:

$$\tau_{delay} = \arg \max_{t \in \mathbb{R}} ((s_1 * s_2)(t)), \quad (3)$$

2.2.4 PCG Delay Calculation Method

The PCG signals are relatively complicated and not regular as ECG. Thus using the CC method will cause a significant estimation error. Therefore, the delays are calculated directly by the difference of the key points. The error is reduced by calculating the mean of the five heart cycles. According to the extracted data in Table 1, the calculated delays are shown in Figure 4.

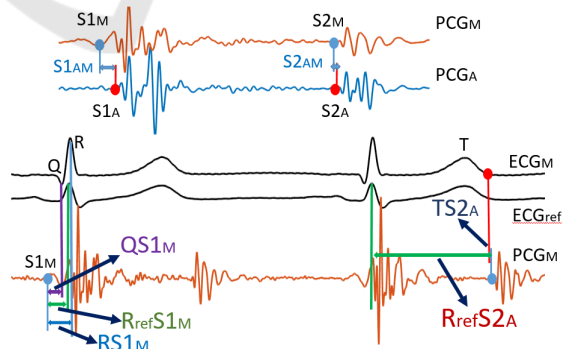


Figure 4: The calculated delays associated with PCG.

$S1_{AM(A, P, T)}$ are the delays between S1 onset in site A and the other auscultation sites. $S2_{AM(A, P, T)}$ are the delays between S2 onset in site A and the other auscultation sites. $RS1_{M(A, P, T)}$ are the delays between S1 onset and R peak in each auscultation site. $R_{ref}S1_{M(A, P, T)}$ are the delays between S1 onset and

R peak in reference ECG. $QS1_{M(A, P, T)}$ are the delays between S1 onset and Q point in each auscultation site. $R_{ref}S2_{A(P, T, M)}$ are the delays between S2 onset and R peak in reference ECG. $TS2_{A(P, T, M)}$ are the delays between S2 onset and T wave ending in each auscultation site.

3 RESULTS

3.1 The Effect of IED on ECG Delays

Figure 5 shows the IED of 5 cm and 15 cm compared with 10 cm. The delays of the occurrence of R peak are all close to 0 ms (mean \pm standard deviation; 5cm: -0.359 ± 2.181 ms, 15cm: 0.805 ± 1.861 ms), except one outlier. Therefore, we can basically conclude that the IED does not affect the R peak occurrence significantly, and there is no obvious regularity in the effect.

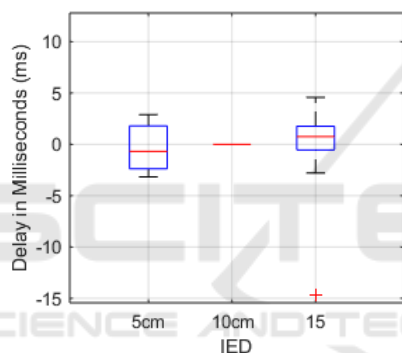


Figure 5: IED caused ECG delay (10 cm as reference).

3.2 Delay between Standard Lead I ECG and Site Specific ECG

As shown in Figure 6, the delay between auscultation sites shows an increasing trend from site A to site M. Compared with the standard lead I ECG, the ECG at A site is normally negative, which means the R peaks at site A is advanced, R peaks at P and T are close to standard lead I ECG; and R peak at M comes later than standard lead I ECG.

3.3 PCG Delay between Site A and the Rest

For the PCG delay between the auscultation sites (site A is as the reference), S1 and S2 are analysed separately. The results are shown in Figure 7. S1 onset becomes earlier (negative) from A to M. However, S2 onset almost remains the same from A to T, but there is a slight delay (positive) at M.

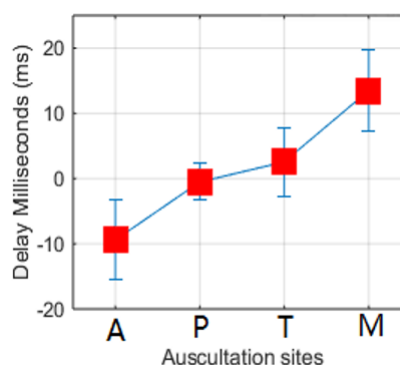


Figure 6: The delay (mean \pm standard deviation, SD) between auscultation sites ECG and standard Lead I.

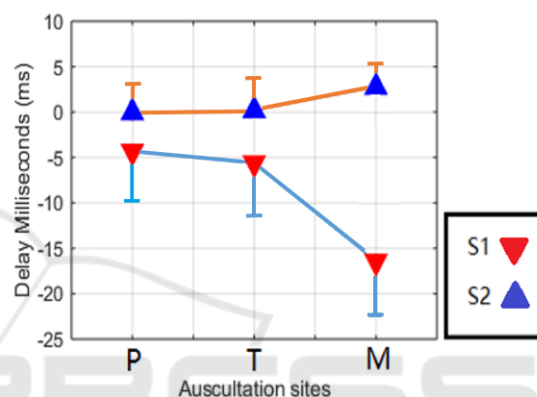


Figure 7: The delay of S1 (red) and S2 (blue) in each auscultation site (A site as reference).

3.4 Delay between ECG and PCG

Figure 8 shows the delay between S1 onset in each auscultation site and R peak in standard Lead I ECG. The delay trend is similar to the S1 onset delay trend, but it can be seen that at site A, the onset of S1 occurs after R-peak. When it comes to site M, the S1 onset is basically before R-peak. Figure 9 illustrates the delay of S1 onset, R-peak and Q point in the auscultation site ECG. The delay trend is similar to the delay of Standard Lead I, but it becomes larger. At site A and M, there are average 20 ms time difference between S1 onset and R-peak. However, compared with Q point, the average delay in site M is close to 0.

S2 is widely regarded as occurring right after T-wave. In this study, it is found that the S2 onsets are basically after T wave ending points in auscultation area, except 4 groups of outlier as shown in Figure 10. Besides, the relationship between Lead I ECG R-peak and S2 onset is also presented in Figure 11.

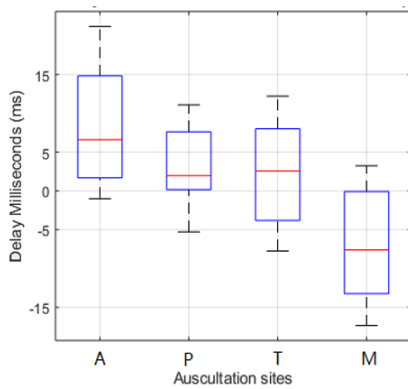


Figure 8: The delay between S1 onset for each auscultation site and R peak in standard Lead I.

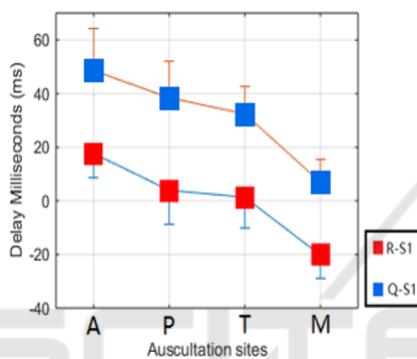


Figure 9: The delay between S1 onset and R peak/ Q point in each auscultation site.

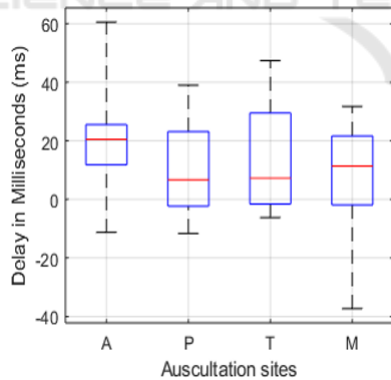


Figure 10: The delay between S2 onset and T wave ending point in each auscultation site.

4 DISCUSSION

This study aimed to analyse the time delay between ECG and PCG at different auscultation sites (A, P, T, M), and investigated the changes in the time occurrence of the R-peak in relation to the distance between the recording electrodes. The results shown

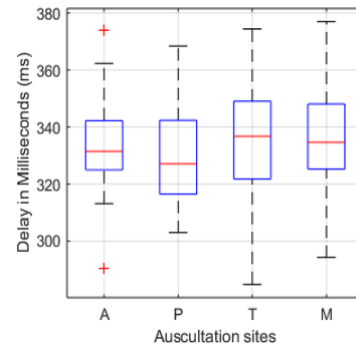


Figure 11: The delay between S2 onset and R peak in Standard Lead I.

firstly that the time property for PCG segmentation based on ECG in the previous study can be misleading and holds only for specific auscultation sites. In our recorded PCG signals, the S1 onset was gradually advanced from auscultation site A to site M, while the S2 was delayed in the meantime. This result is basically in line with our previous knowledge that S1 is generated at heart apex (site M and T) and S2 is generated at heart base (site A and P) (Karnath and Thornton, 2002), so S1 should be captured at site M earlier and S2 should be captured at site A earlier. As the result of heart sound propagation variation on the chest, the S1 onsets in the captured PCG can occur before or after R peak in the ECG. Normally, the S1 onset is after R peak at site A, before R peak at site M, and adjacent to R peak at site P and T. Therefore, distinguishing the auscultation location is necessary for doing more precise segmentation.

Secondly, there is regularity in the translation of the R-peak relative to the auscultation sites. Considering the body as a volume conductor, we can conclude the R-peak of the ECG signals is conducted from site A to site M. Because site T and M coincide with the chest lead in clinic, we also analyzed the open-source 12 leads ECG, and found analogous delay trend between V2 to V6. This finding is similar to the electrical axis caused QRS complex deviation, and the direction is reverse for PCG and thus care should be taken when using the ECG as a reference signal to segment the PCG. When the signal is captured at site M where S1 onset is far before R peak, Q point can be an alternative reference point for the segmentation.

Thirdly, the IED has not effect on the R peak shifting. Thus, shortening the IED can be of help to reduce the size when designing ECG-PCG integrated small device.

Besides, it is found that the RSR' (An ECG finding in which there are two R waves) happened in 5 subjects' site A ECG during the experiment. Normally the RSR' occurs in the conditions of right bun-

dle branch block (RBBB) or left bundle branch block (LBBB) (Daniela, 1996), but there is no such physiological or heart conditions on the subjects. Therefore, it worth noticing to choose appropriate R peak when using ECG to do PCG segmentation under this condition. In our analysis, the first peak was used in the delay calculation and it conforms to the rest trend.

Lastly, there are also some limitations in this study. The IED effects on ECG were tested by only 5 cm, 10 cm and 15cm which was limited by the diameter of the electrodes (4 cm). If there are more interpolations between them, the result will be more convincing and accurate. In the analysis of IED effect on ECG, there is one outlier with around 15 ms R peak shifting cannot be explained. It is conjectured that the error was caused by the misplacement of the electrodes.

5 CONCLUSIONS

The study found that when the ECG is captured at auscultation sites, the R peak of ECG shifted backward regularly from A to M, and the distance between the electrodes did not affect the R peak shifting. In addition, the propagation of the heart sound on the chest caused a delay on S1 onset in the captured PCG signals. Therefore, the R peak shifting and PCG delay lead that using R peak to directly locate S1 in PCG no longer accurate. This can be improved by distinguishing the time property of each auscultation site. All the findings will be of help in designing small ECG-PCG integrated device, and providing theoretical basis for using ECG to do more accurate PCG segmentation.

REFERENCES

Ahlström, C. (2006). *Processing of the Phonocardiographic Signal: methods for the intelligent stethoscope*. PhD thesis, Institutionen för medicinsk teknik.

Andresen, A., Galen, P., Warner, R., and Selvester, R. (2006). Combined ecg and sound chart report and methodology. US Patent App. 11/140,010.

Auer, R., Bauer, D. C., Marques-Vidal, P., Butler, J., Min, L. J., Cornuz, J., Satterfield, S., Newman, A. B., Vittinghoff, E., Rodondi, N., et al. (2012). Association of major and minor ecg abnormalities with coronary heart disease events. *Jama*, 307(14):1497–1505.

Bahadirlar, Y. and Gülçür, H. Ö. (2000). Cardiac passive acoustic localization: Cardiopal. *Turkish Journal of Electrical Engineering & Computer Sciences*, 6(3):243–260.

Cozic, M., Durand, L.-G., and Guardo, R. (1998). Development of a cardiac acoustic mapping system.

Medical and Biological Engineering and Computing, 36(4):431–437.

Daniela, T. (1996). Clinical characteristics and prognosis significance of bundle-branch block (bbb) associated with acute myocardial infarction (ami). *Rom J Intern Med*, 34(3-4):211–215.

El-Segaier, M., Lilja, O., Lukkarinen, S., Sörnmo, L., Sepponen, R., and Pesonen, E. (2005). Computer-based detection and analysis of heart sound and murmur. *Annals of Biomedical Engineering*, 33(7):937–942.

Homaeinezhad, M., Sabetian, P., Feizollahi, A., Ghafari, A., and Rahmani, R. (2012). Parametric modelling of cardiac system multiple measurement signals: an open-source computer framework for performance evaluation of ecg, pcg and abp event detectors. *Journal of medical engineering & technology*, 36(2):117–134.

Iwata, A., Ishii, N., Suzumura, N., and Ikegaya, K. (1980). Algorithm for detecting the first and the second heart sounds by spectral tracking. *Medical and Biological Engineering and Computing*, 18(1):19–26.

Kang, S., Doroshov, R., McConnaughey, J., Khandoker, A., and Shekhar, R. (2015). Heart sound segmentation toward automated heart murmur classification in pediatric patents. In *2015 8th International Conference on Signal Processing, Image Processing and Pattern Recognition (SIP)*, pages 9–12. IEEE.

Kania, M., Rix, H., Fereniec, M., Zavala-Fernandez, H., Janusek, D., Mroczka, T., Stix, G., and Maniewski, R. (2014). The effect of precordial lead displacement on ecg morphology. *Medical & biological engineering & computing*, 52(2):109–119.

Karnath, B. and Thornton, W. (2002). Auscultation of the heart. *Hospital Physician*, 38(9):39–45.

Kumar, D., Carvalho, P. d., Antunes, M., Henriques, J., Maldonado, M., Schmidt, R., and Habetha, J. (2006). Wavelet transform and simplicity based heart murmur segmentation. In *2006 Computers in Cardiology*, pages 173–176. IEEE.

Laguna, P., Jané, R., and Caminal, P. (1992). Adaptive filtering of ecg baseline wander. In *1992 14th Annual International Conference of the IEEE Engineering in Medicine and Biology Society*, volume 2, pages 508–509.

Lehner, R. J. and Rangayyan, R. M. (1987). A three-channel microcomputer system for segmentation and characterization of the phonocardiogram. *IEEE Transactions on Biomedical Engineering*, (6):485–489.

Liang, H., Lukkarinen, S., and Hartimo, I. (1997). Heart sound segmentation algorithm based on heart sound envelopegram. In *Computers in Cardiology 1997*, pages 105–108. IEEE.

Liang, H., Lukkarinen, S., and Hartimo, I. (1998). A boundary modification method for heart sound segmentation algorithm. In *Computers in Cardiology 1998. Vol. 25 (Cat. No. 98CH36292)*, pages 593–595. IEEE.

Lima, C. S. and Cardoso, M. J. (2007). Phonocardiogram segmentation by using hidden markov models.

Nogata, F., Yokota, Y., Kawamura, Y., Morita, H., and Uno, Y. (2012). Novel technique for visualizing heart mo-

- tion without using ultrasonic cardiography. In *Proceedings of 2012 IEEE-EMBS International Conference on Biomedical and Health Informatics*, pages 249–252. IEEE.
- Okada, M. (1982). Chest wall maps of heart sounds and murmurs. *Computers and biomedical research*, 15(3):281–294.
- O’Keefe Jr, J. H., Hammill, S. C., Freed, M. S., and Pogwizd, S. M. (2010). *The complete guide to ECGs*. Jones & Bartlett Publishers.
- Ölmez, T. and Dokur, Z. (2003). Classification of heart sounds using an artificial neural network. *Pattern Recognition Letters*, 24(1-3):617–629.
- Oskeeper, T. and Watrous, R. (2002). Detection of the first heart sound using a time-delay neural network. In *Computers in Cardiology*, pages 537–540. IEEE.
- Pan, J. and Tompkins, W. J. (1985). A real-time qrs detection algorithm. *IEEE Trans. Biomed. Eng.*, 32(3):230–236.
- Phanphaisarn, W., Roeksabutr, A., Wardkein, P., Koseeyaporn, J., and Yupapin, P. (2011). Heart detection and diagnosis based on ecg and epcg relationships. *Medical devices (Auckland, NZ)*, 4:133.
- Ricciardi, D., Cavallari, I., Creta, A., Giovanni, G. D., Calabrese, V., Belardino, N. D., Mega, S., Colaioni, I., Ragni, L., Proscia, C., Nenna, A., and Sciascio, G. D. (2016). Impact of the high-frequency cutoff of band-pass filtering on ecg quality and clinical interpretation: A comparison between 40hz and 150hz cutoff in a surgical preoperative adult outpatient population. *Journal of Electrocardiology*, 49(5):691 – 695.
- Ricke, A. D., Povinelli, R. J., and Johnson, M. T. (2005). Automatic segmentation of heart sound signals using hidden markov models. In *Computers in Cardiology, 2005*, pages 953–956. IEEE.
- Sapsanis, C., Welsh, N., Pozin, M., Garreau, G., Tognetti, G., Bakhshae, H., Pouliquen, P. O., Mitral, R., Thompson, W. R., and Andreou, A. G. (2018). Stethovest: A simultaneous multichannel wearable system for cardiac acoustic mapping. In *2018 IEEE Biomedical Circuits and Systems Conference (BioCAS)*, pages 1–4. IEEE.
- Schmidt, S. E., Holst-Hansen, C., Graff, C., Toft, E., and Struijk, J. J. (2010). Segmentation of heart sound recordings by a duration-dependent hidden markov model. *Physiological measurement*, 31(4):513.
- Shino, H., Yoshida, H., Yana, K., Harada, K., Sudoh, J., and Harasewa, E. (1996). Detection and classification of systolic murmur for phonocardiogram screening. In *Proceedings of 18th Annual International Conference of the IEEE Engineering in Medicine and Biology Society*, volume 1, pages 123–124. IEEE.
- Syed, Z., Gutttag, J., Levine, R., Nesta, F., and Curtis, D. (2004). Automated auscultation system. US Patent App. 10/464,267.
- Wang, X., Li, Y., Sun, C., and Liu, C. (2009). Detection of the first and second heart sound using heart sound energy. In *2009 2nd International Conference on Biomedical Engineering and Informatics*, pages 1–4. IEEE.
- Wartak, J. (1972). *Phonocardiology; integrated study of heart sounds and murmurs*. HarperCollins Publishers.
- Zarrabi, M., Parsaei, H., Boostani, R., Zare, A., Dorfeshan, Z., Zarrabi, K., and Kojuri, J. (2017). A system for accurately predicting the risk of myocardial infarction using pcg, ecg and clinical features. *Biomedical Engineering: Applications, Basis and Communications*, 29(03):1750023.
- Zhong, L., Guo, X., Ji, A., and Ding, X. (2011). A robust envelope extraction algorithm for cardiac sound signal segmentation. In *2011 5th International Conference on Bioinformatics and Biomedical Engineering*, pages 1–5. IEEE.